Eur. J Mineral.
1991, 3, 507-525

Tertiary nephelinitic magmatism in Eastern Paraguay : Petrology, Sr-Nd isotopes and genetic relationships with associated spinel-peridotite xenoliths.

PIERO COMIN-CHIARAMONTI[1, *], LUCIA CIVETTA[2], RICCARDO PETRINI[3], ENZO MICHELE PICCIRILLO[4], GIULIANO BELLIENI[5], PAOLO CENSI[1], PETER BITSCHENE[6], GABRIELLA DEMARCHI[4], ANGELO DE MIN[4], CELSO DE BARRO GOMES[4, **], ANA MARIA CASTILLO[7] and JUAN CARLOS VELAZQUEZ[7].

[1] Istituto di Mineralogia, Petrografia e Geochimica, Università di Palermo, Via Archirafi 36, 90123 Palermo, Italy

[2] Dipartimento di Geofisica e Vulcanologia, Università di Napoli, Largo S. Marcellino 10, 80138 Napoli, Italy

[3] Istituto di Geocronologia e Geochimica Isotopica, Consiglio Nazionale delle Ricerche, Via Cardinale Maffi 36, 56100 Pisa, Italy

[4] Istituto di Mineralogia e Petrografia, Università di Trieste, Piazzale Europa 1, 34100 Trieste, Italy

[5] Dipartimento di Mineralogia e Petrologia, Università di Padova, Corso Garibaldi 37, 35137 Padova, Italy

[6] Institut für Mineralogie, Ruhr-Universität, Postfach 102148, 4630 Bochum, W-Germany

[7] Instituto de Ciencias Bàsicas, Universidad Nacionál de Asunción, Ciudád Universitaria, San Lorenzo, Asunción, Paraguay

[*] Permanent address : Istituto di Mineralogia e Petrografia dell'Università, Piazzale Europa 1, I-34100 Trieste, Italy.

[**] Permanent address : Instituto de Geociências, Universidade de Sao Paulo, Caixa Postal 20899, 01498 Sao Paulo, Brazil.

Abstract : Plugs, flows and dykes of nephelinitic (and ankaramitic) rocks occur near Asunción (Eastern Paraguay ; 61-39 Ma). This magmatism occurs at the western boundary of the Paraná basin and is associated with NW-SE-trending rift and antiform structures. Nephelinites contain variable amounts of crustal (sedimentary, metamorphic and volcanic) and mantle (spinel-peridotite) xenoliths.

The genesis of the Asunción nephelinites requires a mantle source geochemically and isotopically distinct from that represented by the spinel-peridotite nodules included in the lavas. The most likely mantle source is a garnet peridotite characterized by small-scale heterogeneities, at least in terms of Sr and Nd isotopes. This mantle source was subjected to (1) low degrees of partial melting (*e.g.* 3 - 4 %), (2) enrichment in Nb, Ba, La, Ce, Sr and P relative to a primordial mantle.

It is suggested that the enrichment in incompatible elements may be due to metasomatic processes related to a thermal anomaly responsible for the generation of the Lower Cretaceous Paraná flood lavas.

The initial Sr isotope ratios of the Asunción nephelinites (R_0 = 0.7036-0.7039) indicate a mantle source distinct from that of the Lower Cretaceous magmatism (Central-Eastern Paraguay : alkaline magmatism, R_0 = 0.7073 ; tholeiitic flood basalts, R_0 = 0.7059).

0935-1221/91/0003-0507 $ 4.75

On the whole, the Cretaceous-Tertiary alkaline and ultra-alkaline magmatism of Central-Eastern Paraguay appears closely linked to rift structures trending NW-SE and WNW-ESE. This may be an indication of a tectono-magmatic event(s) associated with stress-regime changes during the South America-Africa continental separation.

Key-words : Eastern Paraguay, South America, Tertiary nephelinites, Mantle source, metasomatism, partial melting, Sr-Nd isotopes.

Introduction

Nephelinitic plugs, flows and dykes dominate the Tertiary (61-39 Ma) magmatism in Eastern Paraguay, near Asunción (Fig. 1 ; Bitschene, 1987). This magmatism is controlled by NW-SE- trending rift structures, and represents the most recent alkaline activity on the western border of the Paranà basin (Livieres & Quade, 1987). In this area a tephritic-phonolitic magmatism of Upper Permian to Upper Cretaceous age is also present (240-108 Ma ; Comin-Chiaramonti *et al.*, 1990), locally associated with Cretaceous carbonatites (130-86 Ma ; Eby & Mariano, 1986). Note that an important alkaline magmatism of lower Cretaceous to Eocene age (135 to 45 Ma ; Gomes *et al.*, 1990) is also widespread around the eastern margin of the northern Paranà Basin (Fig. 1A).

The investigated Tertiary nephelinites are important since they represent an ultra-alkaline (Le Bas, 1987) magmatism that occurred inland long after the South America - Africa continental separation. Also, they contain spinel-peridotite xenoliths strongly enriched in incompatible elements (Comin-Chiaramonti *et al.*, 1986 ; Demarchi *et al.*, 1988).

The present paper addresses (1) petrological, geochemical and Sr-Nd isotope aspect bearing on the origin of nephelinite, (2) petrogenetic relationships between nephelinites and the enclosed mantle xenoliths, and (3) Sr-Nd isotope characteristics of the subcontinental mantle sources involved in the generation of the alkaline and tholeiitic magmas of the Paraná Basin.

Fig. 1. A : Sketch map showing the post-Palaeozoic occurrences -squares and circles- of alkaline rock-types at the border of and within the Paraná Basin -squares and circles- (after Gomes *et al.*, 1990). 1 : pre-Devonian crystalline basement ; 2 : pre-volcanic sediments (mainly Palaeozoic) ; 3 : flood volcanics of the Serra Geral Formation (Lower Cretaceous) ; 4 : post volcanic sediments (mainly Upper Cretaceous) ; 5 : syncline-type structure ; 6 : arch-type structure ; 7 : flexure-type structure ; 8 : major structural lineament.

B : Simplified structural map of Eastern Paraguay. 1 : antiform-type structure ; 2 : synform-type structure ; 3 : major faults ; 4 : major structural lineaments. Stippled area indicates the extension of the stratoid tholeiitic volcanic rocks of the Serra Geral Formation, Eastern Paraguay (from Livieres & Quade, 1987 and Bellieni *et al.*, 1986, modified). Dotted areas indicate the main occurrences of alkaline rock-types.

C : Simplified geological map of the Ypacaray Valley and adjacent areas (Degraff *et al.*, 1981). PC, Precambrian , LS and US, Lower and Upper Silurian, respectively ; J, Jurassic-Cretaceous , T, Tertiary nephelinitic occurrences (unconformable on the Jurassic red sandstones of the Misiones Formation) ; f, major faults.

1) Cerro Verde. Small plug (about 300 m in diameter and 20 m high) containing rare mantle (up to 2 cm across) and very abundant crustal (up to 100 cm across) xenoliths.

2) Limpio. Lava flow (about 8 m thick) with scarce mantle (up to 2 cm diam.) and crustal (up to 25 cm diam.) xenoliths.

3) Remanso Castillo. Subvertical NW-SE trending dyke, 5 m thick.

4) Nueva Teblada. Lava flow (about 10 m thick) with abundant mantle xenoliths up to 20 cm across.

5) Tacumbú. Small plug (about 200 m in diameter and 50 m high), which yields abundant mantle and rare crustal xenoliths (up to 7 cm and up to 50 cm across, respectively).

6) Lambaré. Small plug (about 170 m in diameter and 55 m high) with abundant mantle xenoliths (up to 10 cm across) and rare crustal xenoliths (up to 30 cm in size).

7) Cerro Patiño. Very small plug (?) with crustal xenoliths (up to 50 cm) and rare mantle xenoliths (up 2 cm across).

8) Nemby. Plug (900 x 500 m, and 80 m above the plain) with very abundant mantle xenoliths (*ca.* 10-15 % by volume and up to 40 cm across) and rare crustal xenoliths (up to 100 cm across).

Analytical procedures

Major and trace element contents of whole-rocks were determined by X-ray fluorescence (Bellieni *et al.*, 1983) ; microprobe mineral compositions were analysed according to Comin-Chiaramonti *et al.* (1986).

Sr isotope compositions were measured after Sr separation by standard ion-exchange chromatography. The measured $^{87}Sr/^{86}Sr$ ratios were frationation-corrected to an $^{86}Sr/^{88}Sr$ value of 0.1194. Repeated analyses of the NBS 987 Sr standard gave average $^{87}Sr/^{86}Sr$ ratios of 0.71027±3. Standard deviations are expressed as 2σ on the mean.

Nd isotope composition analyses were carried out following the chemical and spectrometric procedures described in Zindler *et al.* (1979). The $^{143}Nd/^{144}Nd$ measured ratios were corrected for fractionation to $^{146}Nd/^{144}Nd$ = 0.7219 and normalized to the La Jolla Nd standard. Standard deviations are expressed as 2σ on the mean.

Carbon isotopic compositions were performed on hand-picked carbonate grains purified in hot distilled water, after vacuum heating at

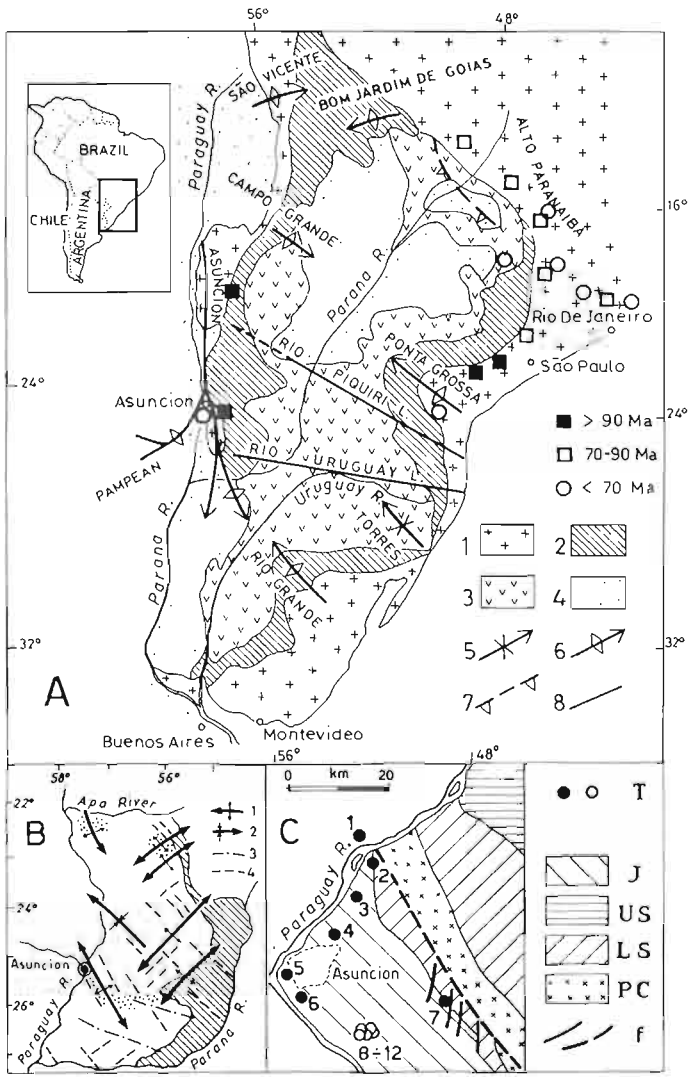

Fig. 1

400°C and reacting with 100 % H_3PO_4 by a Finningan Mat Delta E mass spectrometer. The results are given in δ per mil notation ; PDB-1 is the reference standard ; 1σ standard deviation is 0.05‰.

Petrography and mineral compositions

Nephelinites and ankaramites

The investigated rocks are nephelinites and, subordinately, ankaramites (Fig. 2), according to De La Roche *et al.* (1980) and nephelinites (CIPW Ab < 5 % wt. and Ne > 20 % wt.), according to Le Bas (1989).

Nephelinites and ankaramites are characterized by olivine phenocrysts and microphenocrysts of olivine, clinopyroxene and magnetite set in a microcrystalline groundmass. The latter is made up of clinopyroxene, olivine, opaques, interstitial glass, nepheline and very rare plagioclase microlites. Several samples show poikilitic nepheline, alkali feldspar and carbonates. Some samples contain spinel-peridotite xenoliths (see below) associated with olivine, pyroxene and/or spinel xenocrysts and sometimes also cryptocrystalline materials (sedimentary, metamorphic and volcanic) and quartz xenocrysts derived from the crust (Demarchi *et al.*, 1988).

Modal clinopyroxene (Cpx) ranges from 40 to 49 % (Table 1). *Cpx-microphenocrysts* (0.2-0.5 mm ; Mg# 0.80, Cpx/M in Tables 1, 2) are zoned and range in colour from greenish yellow (core) to pink (rim) ; *groundmass-Cpx* (< 0.2 mm ; Mg# 0.75, Cpx/G in Tables 1, 2) is stubby prismatic and ranges from pale yellow to pink in colour. Compositionally, both micro-

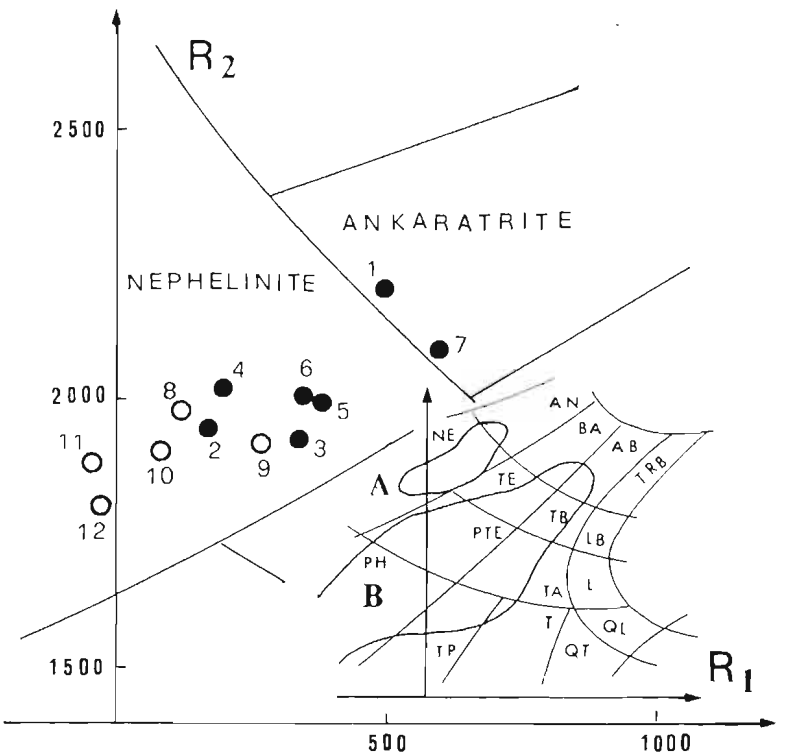

Fig. 2. Plot of the investigated nephelinites of Eastern Paraguay (*cf.* Table 3) in the diagram of De La Roche *et al.* (1980). Circles : Nemby nephelinites, solid circles : other Asunción nephelinites. In inset : A, field of Tertiary ultra-alkaline rocks of the Asunción area and B, field of Mesozoic alkaline rocks of Central-Eastern Paraguay, SW of the Asunción area (Comin-Chiaramonti *et al.*, 1990). R1 = 4Si – 11(Na+K) – 2(Fe+Ti) , R2 = 6Ca + 2Mg + Al.

phenocrystic and groundmass Cpx correspond to salites (Fig. 3), the latter having higher Fe/Mg ratio. *Clinopyroxene xenocrysts* (0.3-2 mm ; Mg# 0.93, Cpx/X in Tables 1, 2) occasionally show spinel exsolutions and glassy inclusions. These clinopyroxenes (diopsides, Fig. 3) are compositionally similar to the Cpx of the peridotite xenoliths. Rare *orthopyroxene xenocrysts* (Mg# 0.92 ; Opx/X in Table 2) are occasionally present.

Modal olivine (Ol) ranges from 7 to 16 % vol. (Table 1). *Ol-phenocrysts* (Fo 89-85 ; Ol/P in Tables 1, 2) are euhedral and fractured (1-7 % vol. ; 0.5-2 mm). *Ol-microphenocrysts* (Fo 82-77 ; Ol/M in Tables 1, 2) are euhedral (1-6 % vol. ; 0.2-0.5 mm) ; *groundmass olivine* (Fo 76-74 ; 3-6 % vol. ; Ol/G in Tables 1, 2) shows euhedral to subhedral outlines. *Olivine xenocrysts* and the olivine of the peridotite xenoliths have the same composition (Fo 93-90).

Ti-magnetite occurs as anhedral microphenocrysts (0.1 - 0.2 mm ; 0.3 - 0.7 % vol. ; Mt/M in Tables 1, 2) and as groundmass phase (< 0.1 mm ; 4 - 7 % vol. ; Mt/G in Tables 1, 2). *Spinel xenocrysts* (Cr/(Cr + Al) = 0.12-0.40, close to the range of spinel from mantle xenoliths) with Ti-magnetite rims are occasionally present. Fine needles of *apatite* are common ; *biotite* flakes and *carbonate* rhombohedra (both < 0.01 mm) are occasionally present in the groundmass.

Mantle xenoliths

Mantle xenoliths (up to 45 cm in size) are spinel lherzolites, harzburgites and dunites (Group 1 of Frey & Prinz, 1978) and correspond to the Cr-diopside series of Wilshire & Shervais (1975). They usually have a protogra-

Table 1. Representative modal analyses (vol. %) and mineral size variation (mm) for nephelinites from Eastern Paraguay.

	1	2	3	4	5	6	7	8	(mm) range
Ol/P	6.5	4.6	2.3	3.8	0.7	4.2		2.6	0.50-2.00
Ol/M	6.2	3.7	2.3	2.9	0.7	2.6	6.5	4.7	0.15-0.50
Ol/G	3.6	3.4	3.8	5.5	5.5	4.3		3.0	0.08-0.15
Cpx/X	1.5	0.5	0.1	0.4	0.9	0.2		0.5	0.28-2.00
Cpx/M	0.9	6.0	1.5	1.4	0.9	0.3	46.3	0.6	0.15-0.50
Cpx/G	46.1	36.6	39.9	44.0	41.3	41.9		39.3	<0.15
Mt/M	0.6	0.3	0.7	0.4	0.7	0.6	5.1	0.3	0.10-0.23
Mt/G	3.9	5.0	6.2	6.8	5.0	5.6		5.0	<0.10
Nepheline	18.8	16.4	17.3	15.3	21.0	20.6	21.4	19.2	
Glass	11.1	22.5	24.8	17.1	22.5	18.7	20.6	21.4	
Apatite	0.5	0.5	0.7	0.1	0.4	0.4	0.1	0.3	<0.10
Biotite	—	—	0.1	—	—	—	—	—	<0.01
Carbonates	—	—	—	—	—	—	—	0.1	0.02-0.10
Pl	—	—	0.2	—	—	—	—	—	0.02-0.10
Xenoliths	0.3	0.5	0.1	2.3	0.4	0.6	—	3.0	0.13-1.55

Numbers as in Fig. 1. Ol, olivine ; Cpx, clinopyroxene ; Mt, magnetite ; Pl, plagioclase. X, xenocrysts ; P, phenocrysts ; M, microphenocrysts ; G, groundmass.

Table 2. Average microprobe analyses of clinopyroxenes (Cpx), orthopyroxenes (Opx), olivines (Ol), magnetite (Mt) and nepheline.

	Cpx				Opx	Ol				Mt		Nepheline
	N	X	M	G	X	N	P	M	G	M	G	
SiO_2	55.13	54.16	47.87	45.30	54.84	41.19	40.30	38.66	38.09	—	—	41.94
TiO_2	0.10	0.12	2.28	3.61	0.00	—	—	—	—	18.92	20.99	—
Al_2O_3	1.48	2.72	6.20	8.07	4.80	—	—	—	—	6.47	4.56	35.09
FeO_t	2.33	2.33	6.27	7.40	5.18	8.59	11.14	19.12	22.21	66.25	67.22	—
MnO	0.16	0.11	0.17	0.10	0.14	0.11	0.20	0.47	0.66	0.86	0.96	—
MgO	17.66	17.00	14.15	12.33	32.92	49.64	47.78	41.09	38.37	3.62	2.83	—
CaO	21.90	21.72	22.05	22.61	1.17	0.02	0.09	0.51	0.59	—	—	0.91
Na_2O	0.99	0.91	0.50	0.23	0.01	—	—	—	—	—	—	18.26
K_2O	0.00	0.00	0.00	0.04	0.00	—	—	—	—	—	—	4.47
Cr_2O_3	0.85	0.85	0.29	0.12	0.92	—	—	—	—	1.37	0.81	—
NiO	—	—	—	—	—	0.40	0.26	0.16	0.11	—	—	—
SUM	100.60	99.92	99.78	99.81	99.98	99.95	99.90	100.01	100.03	97.49	97.37	100.67
Si	1.979	1.959	1.770	1.694	1.891	1.002	0.999	0.992	0.993	—	—	1.003
Ti	0.003	0.003	0.063	0.102	0.000	—	—	—	—	0.505	0.570	—
Al^{iv}	0.021	0.041	0.230	0.306	0.109	—	—	—	—	—	—	0.987
Al^{vi}	0.042	0.075	0.040	0.050	0.086	—	—	—	—	—	—	—
Fe^{3+}	0.018	0.000	0.091	0.066	0.000	0.000	0.003	0.017	0.014	0.680	0.642	—
Fe^{2+}	0.052	0.070	0.103	0.166	0.149	0.174	0.227	0.394	0.470	1.286	1.387	—
Mn	0.005	0.003	0.005	0.003	0.004	0.002	0.004	0.010	0.015	0.026	0.029	—
Mg	0.945	0.917	0.780	0.687	1.691	1.811	1.758	1.571	1.490	0.193	0.154	—
Ca	0.843	0.842	0.873	0.906	0.043	0.001	0.002	0.014	0.017	—	—	0.024
Na	0.069	0.064	0.036	0.017	0.001	—	—	—	—	—	—	0.845
K	0.000	0.000	0.000	0.002	0.000	—	—	—	—	—	—	0.136
Cr	0.024	0.024	0.008	0.004	0.025	—	—	—	—	0.038	0.023	—
Ni	—	—	—	—	—	0.008	0.005	0.003	0.002	—	—	—
Al	—	—	—	—	—	—	—	—	—	0.271	0.194	—
O	6.000	6.000	6.000	6.000	6.000	4.000	4.000	4.000	4.000	4.000	4.000	4.000

Total iron as FeO. N = xenoliths , X = xenocrysts ; P = phenocrysts ; M = microphenocrysts ; G = groundmass.

nular texture (Mercier & Nicolas, 1975, nomenclature). No lava contamination is apparent from petrographic, mineralogical or chemical studies (Comin-Chiaramonti *et al.*, 1986 ; Demarchi *et al.*, 1988). Mantle xenoliths contain variable amounts of glassy patches corresponding to the "blebs" of Maaløe & Prinzlau (1979 ; see later).

Clinopyroxene (Mg# 0.91-0.93 ; 1 to 15 % vol.) is compositionally quite homogeneous (Table 3), showing spinel exsolutions and occasional glassy inclusions.

1 *Orthopyroxene* (Mg# 0.91-0.92 ; 3 to 26 % vol.) is unzoned (Table 3) and rarely shows spinel exsolutions. *Olivine* (60 to 97 % vol.) varies in composition from Fo_{90} (lherzolites) to Fo_{93} (dunites) (Table 3). *Spinel* (Cr/(Cr + Al) 0.10-0.60 ; 0.6 to 4 % vol. ; Table 3) may be surrounded by microcrystalline glassy rims and "blebs".

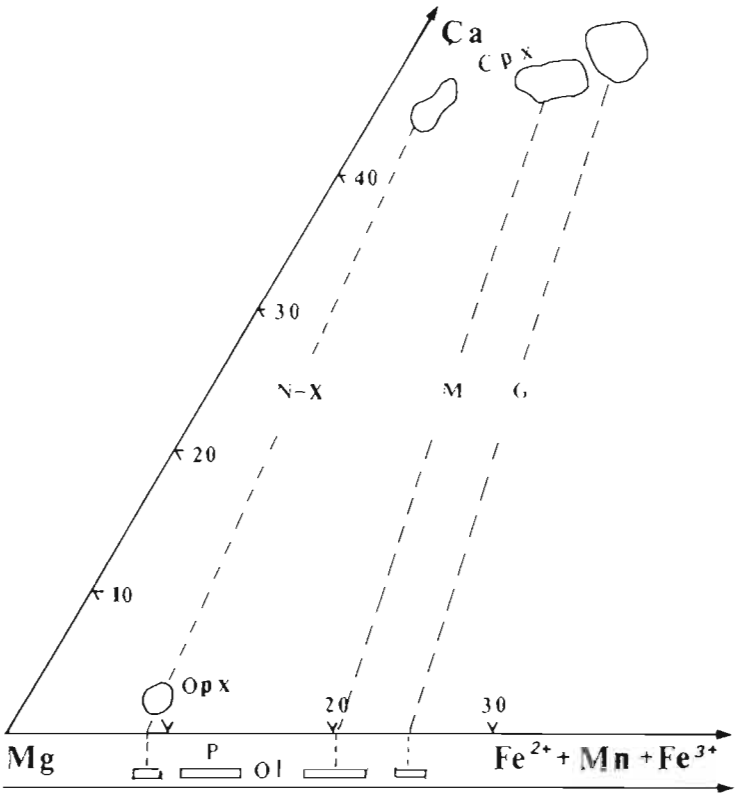

Fig. 3. Compositional variation of clinopyroxene, olivine and orthopyroxene in the Ca–Mg– (Fe^{2+} + Mn + Fe^{3+}) conventional diagram (atoms %). N = xenoliths and microxenoliths ; X = xenoliths and microxenoliths , X = xenocrysts ; M= microphenocrysts ; G = groundmass phases.

Pyrrhotite, pentlandite and *apatite* occur as dispersed grains. Very rare *carbonate* may be present as tiny euhedral crystals. The "residual" character of the whole assemblage is reflected by the compositional variation of each mineral phase (Demarchi *et al.*, 1988), *i.e.*, the Mg/Fe_t (atomic ratio) of the orthopyroxene (9.7 to 11.8) is correlated to the Fo content of the olivine (90 to 93), to the Mg/Fe_t of clinopyroxene (9.2 to 15.3), as well as to the Cr/(Cr + Al) ratio of the spinel (0.10 to 0.60).

The *"blebs"* consist of a glassy matrix containing olivine, clinopyroxene and Cr-spinel microlites. They are considered to have been formed by melting of amphibole and phlogopite (Comin-Chiaramonti *et al.*, 1986).

Equilibration temperatures and pressures of the spinel-peridotite xenoliths (calculated according to Mercier, 1980) vary between 944-1051°C and 14-22 kbar, respectively. Assuming a diameter of 45 cm, corresponding to the size of the largest xenolith, a density of 3.3 g/cm^3 and an origin at a depth of 60 km, the transport of the xenoliths to the surface occurred in less than 10 hours (*cf.* Spera, 1984).

Whole-rock compositions

Nephelinites and ankaramites

The average compositions of the investigated rocks are given in Table 4.

In general, MgO content is negatively correlated with SiO_2, Al_2O_3, Na_2O and K_2O, and is positively correlated with CaO and FeO_t (Fig. 4). The Nemby nephelinites, at similar MgO content, are distinct from the others in having lower TiO_2 and CaO, and higher P_2O_5 and Na_2O contents.

Table 3. Chemical compositions of coexisting phases in bleb-free (BF) and bleb-bearing (BB) xenoliths (after Demarchi *et al.*, 1988) ; amphibole (AMPH) and phlogopite (PHLOG) compositions (from Wilkinson & Le Maitre, 1987) used in the mass balance calculations.

	Ol		Opx		Cpx		Sp		AMPH	PHLOG
BF	3192	3269	3192	3269	3192	3269	3192	3269		
SiO_2	41.23	41.08	56.86	56.60	53.02	53.54			43.98	41.01
TiO_2			0.07	0.02	0.31	0.05	0.06	0.06	0.74	0.18
Al_2O_3			3.33	2.70	5.68	2.70	56.53	41.72	14.10	13.49
FeO_t	9.30	8.05	5.80	5.19	2.57	2.17	10.63	10.65	3.90	2.60
MgO	49.94	50.09	33.77	33.94	15.32	16.62	20.70	18.74	17.99	26.03
CaO	0.03	0.03	0.49	0.47	20.92	21.97			10.75	0.01
Na_2O			0.05		1.47	0.96			3.48	0.32
K_2O					0.01	0.01			0.56	10.00
Cr_2O_3			0.24	0.54	0.82	1.03	12.38	27.58	1.58	0.82
BB	3198	3304	3198	3304	3198	3304	3198	3304	BLEBS	
SiO_2	41.54	40.26	56.04	57.21	51.32	54.76			44.21	
TiO_2			0.05	0.02	0.45	0.03	0.12	0.14	0.45	
Al_2O_3			3.47	1.93	5.84	3.99	57.67	43.54	7.83	
FeO_t	8.91	8.40	5.67	5.33	2.79	2.17	8.98	12.98	6.51	
MgO	49.22	49.38	33.22	34.36	15.42	16.18	20.79	18.94	28.57	
CaO	0.04	0.00	0.57	0.42	20.10	22.76			4.18	
Na_2O			0.05	0.05	1.37	0.94			1.30	
K_2O					0.01	0.01			1.90	
Cr_2O_3			0.24	0.38	0.76	0.87	10.70	24.01	4.00	

Trace-element variations relative to MgO (Fig. 5) display well defined trends in the Nemby samples. These latter show, increasing Sr, Ba, La, Ce, Y and Nb, for decreasing MgO, coupled with decreasing Ni and Cr ; Rb remains virtually constant (av. 59 ± 2 ppm). The nephelinites of the other localities show scattered variations mainly for La, Ce, Zr and Nb. Note that the least differentiated nephelinite (n.1 of Table 4 ; Mg# 0.69) has the highest incompatible element contents.

The compositional variations of the Nemby samples are compatible with fractional crystallization. Mass balance calculations (major elements) show that the transition from sample 8 (Mg# 0.674) to sample 12 (Mg# 0.638) yields $\Sigma res^2 = 0.88$; this requires the extraction of olivine (3.9 % : Ol/P of Table 2), clinopyroxene (9.2 % : Cpx/M of Table 2) and magnetite (2.6 % : Mt/M of table 2). The incompatible trace element calculated/observed ratios (Rayleigh fractionation ; partition coefficients after Bristow, 1984) range, on the whole, between 0.95 and 1.18.

In general, the La/Y ratio of the nephelinites increases with the degree of silica undersaturation, *i.e.* CIPW Ne + Lc + Cs. Note that the nephelinites are strongly enriched in LREE (chondrite normalized values : La = 235-329 ; Ce = 177-245 ; Nd = 82-110) relative to HREE (Yb = 7-11 ; Lu = 7-10, S. Table 4).

Mantle xenoliths

Representative compositions of the mantle xenoliths enclosed in the nephelinites are listed in Table 5. They refer to different peridotite suites with or without "blebs" (BB- and BF-suites, respectively). A detailed discussion of

Table 4. Average analyses of nephelinites from Eastern Paraguay.

	CERRO VERDE	LIMPIO	RINCANSO CASTILLO	NUEVA TEBLADA	TACUMBU	LAMBARE	CERRO PATINO	NEMBY				
	1(n = 2)	2(n = 2)	3(n = 1)	4(n = 2)	5(n = 4)	6(n = 2)	7(n = 1)	8(n = 2)	9(n = 6)	10(n = 14)	11(n = 6)	12(n = 2)
SiO_2	41.52	43.37	44.35	42.83	43.45	42.42	43.81	43.10	44.53	43.78	43.72	44.70
TiO_2	2.68	2.55	2.24	2.18	2.63	2.56	2.38	2.11	2.13	2.20	2.20	2.09
Al_2O_3	12.43	14.00	16.05	13.37	14.85	13.52	14.74	13.46	13.67	14.03	14.30	14.81
FeO_t	11.42	11.08	10.17	11.28	10.55	11.62	10.02	11.13	10.47	10.62	10.60	10.12
MnO	0.24	0.22	0.18	0.24	0.18	0.22	0.18	0.22	0.20	0.22	0.21	0.21
MgO	12.21	9.85	8.03	10.43	9.65	11.19	10.07	10.77	9.99	9.52	9.01	8.69
CaO	12.60	10.90	11.12	11.48	11.28	10.96	12.06	10.87	10.62	10.72	10.70	10.04
Na_2O	4.72	5.80	5.45	5.35	5.17	5.05	5.15	5.75	5.53	5.71	6.02	6.36
K_2O	0.94	1.26	1.48	1.69	1.43	1.29	0.69	1.47	1.71	1.96	1.98	1.78
P_2O_5	1.24	0.97	0.93	1.15	0.81	1.17	0.90	1.12	1.15	1.24	1.26	1.20
Co	54	—	48	—	50	58	46	53	49	—	—	—
Cr	492	389	398	432	377	550	542	609	549	530	515	491
Ni	284	228	154	277	182	320	207	292	277	258	250	254
Ba	1289	1055	1031	1011	1253	1000	1090	1041	1005	1066	1090	1144
Rb	55	38	56	56	71	41	22	60	58	56	60	60
Sr	1278	1109	1102	1079	1104	1081	1016	1061	1089	1116	1123	1150
La	133	107	81	102	84	112	81	112	114	122	122	129
Nd*	—	—	49	—	49	66	49	63	—	—	—	
Ce	192	160	141	185	133	178	145	172	183	191	191	192
Yb*	—	—	1.9	—	1.6	1.9	1.5	1.5	—	—	-	—
Lu*	—	—	0.27	—	0.24	0.28	0.22	0.32	—	—	—	
Zr	307	294	200	286	222	288	165	259	230	237	234	280
Y	27	29	29	25	20	29	26	27	34	34	34	32
Nb	125	93	94	100	90	109	89	95	106	112	113	128
Or	0.00	7.45	8.76	2.15	8.46	7.63	4.08	6.08	10.11	11.31	10.45	10.53
Ab	0.00	1.58	4.28	0.00	0.63	0.08	4.40	0.00	3.42	0.00	0.00	4 51
An	9.94	8.44	14.93	7 45	13.06	10.39	15.04	6.55	7.41	6.84	6.13	6 58
Lc	4.36	0.00	0.00	6.16	0.00	0.00	0.00	2.05	0.00	0 19	0.98	0.00
Ne	21.61	25.70	22.64	24.51	23.34	23.09	21.20	26.34	23.48	26.16	27.58	26.69
Cs	1.12	0.00	0.00	0.00	0 00	0.00	0.00	0.00	0.00	0.00	0.00	0.00
Di	32.93	31.83	27 78	34.01	30.41	29.37	31.40	32.42	30.56	30.99	31.43	28.72
Ol	19.81	15.71	13 18	16.67	15.13	19.56	15.28	17.74	16.24	15.25	14 21	14.22
Mt	2.44	2.36	2.18	2.41	2.26	2.48	2.15	2.38	2.23	2.28	2.26	2.16
Il	5.09	4.85	4.26	4.14	4.99	4.86	4.52	4.01	4.05	4.18	4.18	3.97
Ap	2.93	2.29	2.20	2.72	1.92	2.77	2.13	2.65	2.72	2.93	2.98	2.84
Mg#												
(1)	0.687	0.646	0.619	0.655	0.653	0.664	0.674	0.665	0.662	0.648	0.636	0.638
(2)	0.692	0.651	0.624	0.660	0.658	0.669	0.679	0.670	0.667	0.653	0.641	0.643
Fe_2O_3	6.21	4.56	3.84	4.39	4.47	4.68	3.99	4.45	4.07	4.17	4.09	4.02
FeO	5.48	6.66	6.40	7.06	6.13	6.69	6.13	6.82	6.47	6.54	6.60	6.19
L.O.I.	2.46	2.34	1.99	2.00	2.69	2.11	1.87	2.34	2.06	2.02	2.06	2.07
Sum	99.65	99.48	99.29	99.47	99.33	99.21	99.32	99.62	99.29	99.28	99.26	99.30

Total iron as FeO. Data normalized to 100 % on a volatile-free basis. Fe_2O_3/FeO = 0.17 for CIPW norm calculation ; Mg number (Mg#) = $Mg/(Mg + Fe^{2+})$; Fe_2O_3/FeO ratios of 0.17 for (1) and 0.20, for (2). Original Fe_2O_3, FeO, L.O.I. and sum are also given. Numbers 1 to 8, as in Fig. 1 ; numbers 8 to 12 from Nemby hill, averaged for different MgO contents. * : REE data from Bitschene (1987). Number of analysed samples is given in brackets.

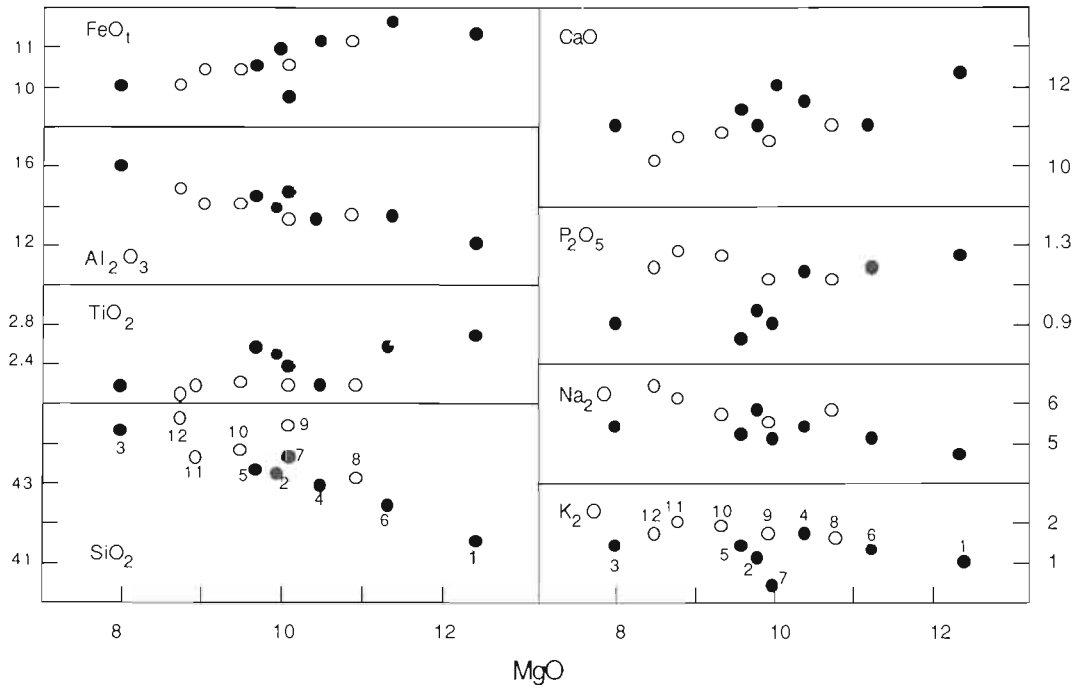

Fig. 4. MgO (wt%) vs. major element (wt%) diagrams for the nephelinites of the Asunción area. Numbers as in Table 4 ; symbols as in Fig. 2

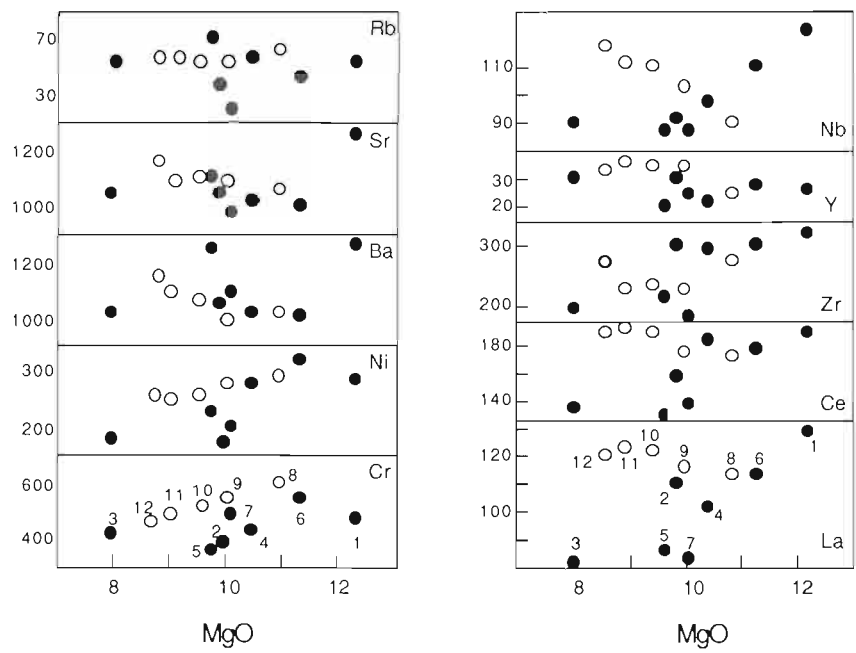

Fig. 5. MgO (wt%) vs. trace element (ppm) diagrams for the nephelinites of the Asunción area. Numbers as in Table 4 ; symbols as in Fig. 2.

Table 5. Representative end-members analyses of BF and BB mantle suites, respectively, from Asunción mantle xenoliths (Demarchi *et al.*, 1988).

	BF Suite		BB suite	
	3192	3269	3198	3304
SiO_2	44.68	43.66	44.97	42.70
TiO_2	0.06	0.01	0.09	0.02
Al_2O_3	2.56	0.77	2.46	1.26
FeO_t	7.88	7.66	7.84	7.82
MnO	0.12	0.11	0.12	0.12
MgO	41.37	46.10	39.93	45.57
CaO	2.27	0.71	3.01	1.01
Na_2O	0.10	0.05	0.26	0.24
K_2O	0.09	0.06	0.43	0.36
P_2O_5	0.02	0.00	0.05	0.04
Cr	2968	2379	2396	3182
Ni	2131	2377	2081	2321
Ba	10	2	31	36
Rb	3	2	7	7
Sr	11	13	44	73
La	3	3	4	3
Ce	5	4	7	5
Zr	13	12	15	12
Y	4	1	5	3
Nb	6	6	7	8

the xenolith compositional variations is given in Comin-Chiaramonti *et al.* (1986) and Demarchi *et al.* (1988). We point out here that "bleb"-bearing xenoliths are significantly enriched in K_2O (up to 0.49 %) and incompatible elements.

Sr, Nd and C isotopes

Initial $^{87}Sr/^{86}Sr$ ratios (R_0) of selected nephelinites range from 0.70362 to 0.70392, while present-day $^{143}Nd/^{144}Nd$ ratios vary from 0.51262 to 0.51280 (Table 6). Samples with low (*e.g.* Limpio) or high (*e.g.* Cerro Verde) contents of crustal xenoliths have very similar R_0 values (*i.e.* 0.70378 and 0.70381, respectively). These data and the absence of significant correlations between R_0 and SiO_2, Rb, K_2O and Ba, as well as their rapid ascent to the surface, suggest that the investigated nephelinites were not appreciably modified by crustal components (*i.e.* granitic components).

The mantle xenoliths enclosed in the nephelinites have Sr and Nd isotopes (Petrini, unpublished data) which differ from those of the nephelinites. These differences are important (*cf.* Fig. 6) and indicate that the mantle source(s) of the nephelinitic magmas was isotopically distinct from that represented by the enclosed mantle xenoliths.

When the R_0 values of the nephelinites are plotted against K/Ar age, a temporal trend becomes apparent (Fig. 7). Between 60 and 40 Ma, R_0 value continuously increases with age, apart from the Cerro Patiño samples. This trend suggests slightly different nephelinite sources.

Carbonate from nephelinites have $\delta^{13}C$ ranging from -5.2 to - 7.9‰ (av. -7.0 ± 0.9 ‰, Table 7), in agreement with an origin from the mantle (-7 ± 1‰ : Pineau & Mathez, 1990).

Discussion and conclusion

In general, there is a consensus that nephelinitic magmas are generated by low degrees of melting and high $CO_2/(CO_2 + H_2O)$ ratios in garnet peridotites which are enriched in incompatible elements prior to or during melting (*e.g.* Eggler, 1978 ; Frey *et al.*, 1978 ; Boettcher *et al.*, 1979 ; Menzies & Murthy, 1980 ; Bristow, 1984 ; Wyllie, 1987).

Spinel peridotites strongly enriched in incompatible elements may also be suitable parental materials for the genesis of strongly alkaline melts (*cf.* Roden *et al.*, 1984 ; Roden, 1987). Thus, it is important to test if at least in terms of major and trace elements the studied nephelinites may have originated from mantle sources similar to those represented by the enclosed spinel-peridotite xenoliths which are enriched in incompatible elements.

The high Mg-number (0.64 - 0.69) and the high Cr (377-609 ppm), Ni (154-320 ppm) and Co (48-58 ppm) contents indicate that the investigated nephelinites approach the composition of a primary magma from the mantle. In fact, it is sufficient to add 3-6 % wt. of olivine Fo_{88} (Ol/P of Table 2) to obtain nephelinites with an Mg-number of 0.71 ("theoretical nephelinite" ; Table 8).

Mass balance calculations, assuming a spinel-lherzolite xenolith strongly enriched in incompatible elements as a mantle source (*i.e.* BB3198 ; mineral and bulk rock compositions

Table 6. Initial $^{87}Sr/^{86}Sr$ (R_0) and present day $^{143}Nd/^{144}Nd$ ratios of selected samples of ultra-alkaline rocks from the Asunción area.

LOCALITY	CERRO VERDE	LIMPIO	LAMBARÉ	NUEVA TEBLADA		NEMBY		TACUMBÚ	REMANSO CASTILLO	CERRO PATINO
AGE (Ma)	57.0±2.3	50.2±1.9	48.9±2.2	46.3±2.0		45.7±1.8		41.3±1.6	40.6±1.6	38.8±2.0
SAMPLE	3080	3082	3097	3103	3209	3213	3283	3068	3083	3399
SiO_2	40.03	41.88	41.05	41.48	42.52	41.91	42.47	41.84	42.98	42.52
TiO_2	2.58	2.46	2.48	2.11	2.05	2.16	2.09	2.53	2.17	2.32
Al_2O_3	11.98	13.52	13.10	12.95	13.41	13.69	13.20	14.30	15.55	14.40
Fe_2O_3	6.27	4.60	4.58	4.48	4.02	3.47	4.07	4.51	3.84	3.99
FeO	5.46	6.64	6.80	7.14	6.48	7.22	6.78	6.17	6.40	6.13
MnO	0.23	0.21	0.21	0.23	0.20	0.20	0.20	0.17	0.18	0.17
MgO	11.77	9.51	10.84	10.10	9.54	8.89	9.88	9.29	7.78	9.77
CaO	12.15	10.52	10.62	11.12	10.45	10.84	10.46	10.86	10.78	11.71
Na_2O	4.55	5.60	4.89	5.18	5.80	5.55	4.62	4.98	5.28	5.00
K_2O	0.91	1.22	1.25	1.64	1.46	1.93	2.26	1.38	1.43	0.67
P_2O_5	1.19	0.94	1.13	1.11	1.18	1.22	1.16	0.78	0.90	0.87
L.O.I.	2.44	2.29	2.05	1.85	2.19	2.12	2.07	2.59	1.99	1.87
Sum	99.56	99.39	99.00	99.39	99.29	99.20	99.26	99.40	99.29	99.32
Co	53	—	57	—	58	—	—	50	48	46
Cr	480	385	544	428	648	539	500	371	398	542
Ni	277	223	317	274	273	242	253	179	154	207
Ba	1258	1050	991	1004	980	990	968	1237	1031	1090
Rb	55	39	41	56	59	50	50	70	56	22
Sr	1278	1111	1070	1066	1013	1030	1063	1082	1102	1016
La	130	105	111	101	116	106	119	82	81	81
Ce	188	157	176	183	176	180	186	131	141	145
Zr	300	288	285	282	234	237	225	218	200	165
Y	27	29	29	25	33	36	33	20	29	26
Nb	122	96	108	99	101	101	105	89	94	89
$R_o(^{87}Sr/^{86}Sr)_o$	0.70381±1	0.70378±1	0.70374±1	0.70369±1	0.70363±1	0.70362±1	0.70369±1	0.70365±3	0.70367±1	0.70392±1
$^{143}Nd/^{144}Nd$	0.512729±6	0.512624±12		0.512803±6 0.512800±20	0.512760±10		0.512655±8	0.512746±6		0.512753±7
Mg#	0.690	0.650	0.676	0.655	0.665	0.644	0.665	0.654	0.624	0.679

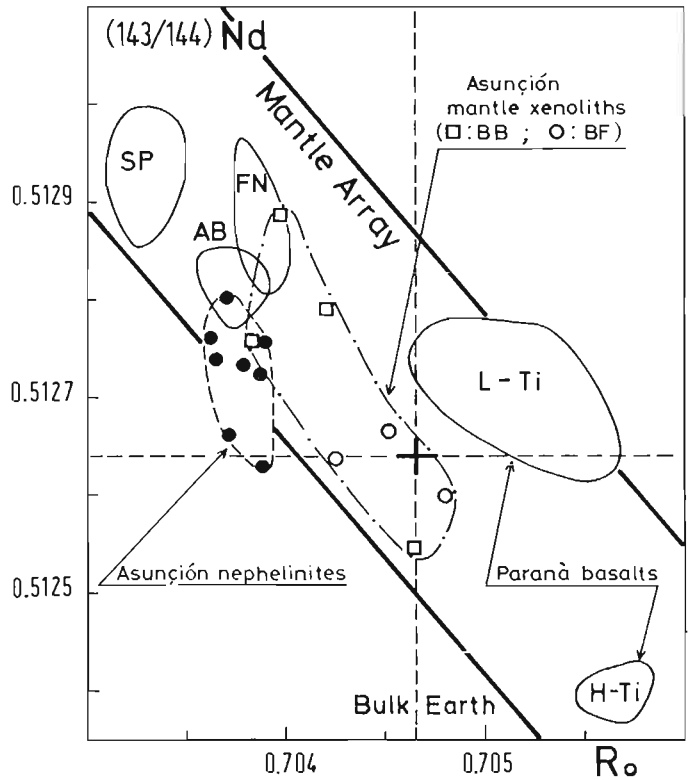

Fig. 6. $^{143}Nd/^{144}Nd$ (present day) vs. R_0 ($^{87}Sr/^{86}Sr$ initial ratios) diagram for Asunción ultra-alkaline rock-types, enclosed mantle-xenoliths (Petrini, unpublished data : BB and BF = Bleb-bearing and Bleb-free suite, respectively) and Mesozoic tholeiitic basalts of Central-Eastern Paraguay (Cordani *et al.*, 1988 , L-Ti and H-Ti : low- and high-titanium suite, respectively). Other fields : SP = St. Paul rocks (Roden *et al.*, 1984) ; FN = Fernando de Noronha, Quixaba Formation (Gerlach *et al.*, 1987) ; AB = Abrolhos (Fodor *et al.*, 1989). R_0 relative to Mantle Array and Bulk Earth (after Faure, 1986) calculated at 41 Ma, assuming Rb/Sr ratio = 0.025 and $^{87}Sr/^{86}Sr$ = 0.7047 for present day Bulk Earth.

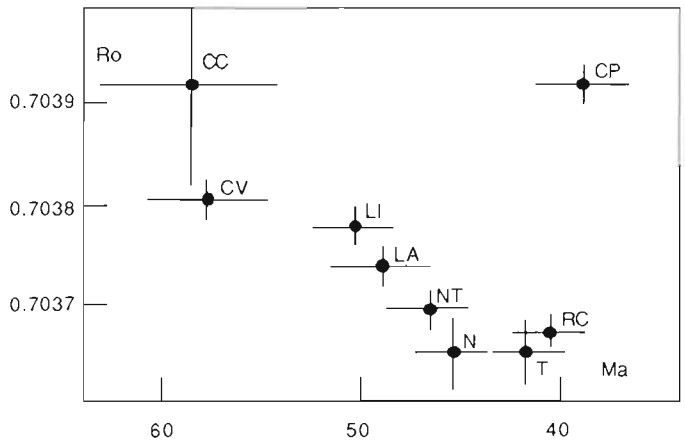

Fig. 7. R_0 vs. age (Ma) diagram (ages after Bitschene, 1987) for nephelinites from the Asunción area. CC, Cerro Confuso phonolitic plug, 2 km south of Cerro Verde hill (R_0 after Bitschene, 1987) ; CV, Cerro Verde ; LI, Limpio ; LA, Lambaré ; NT, Nueva Teblada ; N, Nemby ; T, Tacumbú ; RC, Remanso Castillo ; CP, Cerro Patiño). Bars indicate 2σ for R_0 and 1σ for the age.

Table 7. $\delta^{13}C‰$ (vs PDB-1) values of carbonates from selected nephelinite samples.

Sample	$\delta^{13}C‰$	Sample	$\delta^{13}C‰$
3199	–6.87	3263	–5.22
3213	–7.07	3313A	–7.39
3252	–7.64	3222	–6.87
3260	–7.92	3288	–7.34

Table 8. Calculated "theoretical" parent melts (Mg# 0.71) for Asunción nephelinites (see text for explanation).

	13	14	15	16
SiO_2	41.59	42.31	43.66	42.96
TiO_2	2.61	2.41	2.28	1.99
Al_2O_3	12.12	12.75	14.10	12.70
FeO_t	11.41	11.59	10.07	11.13
MnO	0.24	0.22	0.18	0.22
MgO	13.11	13.31	11.72	12.85
CaO	12.28	10.33	11.54	10.26
Na_2O	4.60	4.76	4.93	5.43
K_2O	0.92	1.22	0.66	1.39
P_2O_5	1.21	1.10	0.86	1.06
Co	57	67	51	61
Cr	515	612	587	676
Ni	358	546	309	492
Ba	1257	943	1043	983
Rb	54	39	21	57
Sr	1246	1019	972	1002
La	130	106	78	106
Ce	188	168	139	163
Zr	300	272	159	245
Y	26	27	25	26
Nb	122	103	85	90

The original nephelinites are from Table 4, and the added olivine (Ol/P) from Table 2. Theoretical nephelinites are the following : n.13 = n.1 + 2.53 % wt Ol ; n.14 = n.5 + 5.77 % wt Ol , n.15 = n.7 + 4.37 % wt Ol ; n.16 = n.8 + 5.63 % wt Ol.

in Tables 3 and 5, respectively), show that the degree of melting necessary to produce a "theoretical nephelinite" ranges from about 5 to 6 %. The best solutions (Σ res^2< 0.2) yield the following solid residua : Ol = 62.4-66.1, Opx = 19.8-20.1, Cpx = 10.3-11.9, Sp = 0.01-0.04, Phlog = 2.6-2.9. The incompatible element contents in the source were calculated using a batch melting equation. The partition coefficients used in the calculations are listed in Table 9.

The results (Fig. 8A) show that the source of the theoretical nephelinite should be enriched (1.5 - 4 times) in Ti, Ba, P, Nb, Ce, La and Zr and depleted in Y relative to the contents in lherzolitic xenoliths enriched in incompatible elements (BB). Thus the Asunción nephelinites cannot be generated by melting of spinel lherzolites of the type represented by the enclosed spinel-lherzolite xenoliths.

As a further test, we assumed that the harzburgitic xenolith BB3304, enriched in incompatible elements (mineral and bulk rock compositions in Tables 3 and 5, respectively), represents a possible mantle residue. The mineral assemblage, calculated from mass balance (Σ res^2 = 0.1), is Ol = 81.3, Opx = 11.7, Cpx = 3.6, Sp = 1.2, Amph = 0.9, and Phlog = 1.3. In this case, assuming 2-6 % melting, the calculated element contents relative to those of the theoretical nephelinites, are distinctly higher (2-3 times) for Ba, P and Ti and lower (by *ca.* 0.5) for Y (*cf.* Fig. 8B). Similar results are also obtained assuming that the lherzolitic xenolith BB3198 is a solid partial melting residue with 2-6 % of melting.

Thus, melting models suggest that it is unlikely that the associated harzburgitic and lherzolitic xenoliths enriched in incompatible elements represent solid partial melting residua related to the generation of the theoretical nephelinite.

Considering garnet-peridotite sources (whole-rock and mineral compositions after Harris *et al.*, 1967 ; Chen, 1971 ; MacGregor, 1977 ; Bristow, 1984 ; Dautria *et al.*, 1987 ; Wilkinson & Le Maitre, 1987) the generation of the Asunción theoretical nephelinites may be modelled for 3-6 % degrees of partial melting for major elements only. Calculated contents of incompatible elements in the source normalized with respect to primordial mantle (Nelson *et al.*, 1986), yield (*e.g.* for 4 % melting) the following enrichment factors : Rb = 1.3-4.4, K = 1-3, Zr = 1-1.9, Sr = 2-3, P = 3.1-4.6, Ce = 3.3-4.5, Ba = 6-9, La = 5-8 and Nb = 8.4-14.

The geochemical and Sr-Nd isotope data, as well as the melting models, show that the Asunción nephelinites are not derived from sources similar to the enclosed spinel-peridotite

Table 9. Solid/liquid partition coefficients used in the melting models.

	Ol	Opx	Cpx	Gar	Sp	Phlog	Amph
Rb	0.0001	0.001	0.025	0.010	0.0001	3.00	0.3
Ba	0.0001	0.010	0.007	0.010	0.0001	1.00	0.4
K	0.0002	0.001	0.0028	0.001	0.0001	10.00	1.0
Nb	0.0010	0.15	0.10	0.10	0.05	1.00	0.5
La	0.00044	0.0005	0.02	0.01	0.029	0.03	0.12
Ce	0.00030	0.0009	0.04	0.021	0.032	0.03	0.20
Sr	0.0010	0.010	0.086	0.010	0.0001	0.10	0.5
P	0.043	0.014	0.009	0.19	0.05	0.20	0.20
Zr	0.01	0.030	0.10	0.155	0.02	0.60	0.35
Ti	0.010	0.100	0.030	0.30	0.10	0.90	0.7
Y	0.0010	0.080	0.367	1.85	0.048	0.03	0.20

Ol, olivine ; Opx, orthopyroxene ; Cpx, clinopyroxene ; Gar, garnet ; Sp, spinel ; Phlog, phlogopite ; Amph, amphibole. Source data : Hanson, 1977 ; Irving, 1978 ; Frey *et al.*, 1978 ; Pearce & Norry, 1979 ; Ottonello *et al.*, 1984 ; Villemant *et al.*, 1981 ; Prinzhofer & Allègre, 1985 ; Ewart & Hawkesworth, 1987.

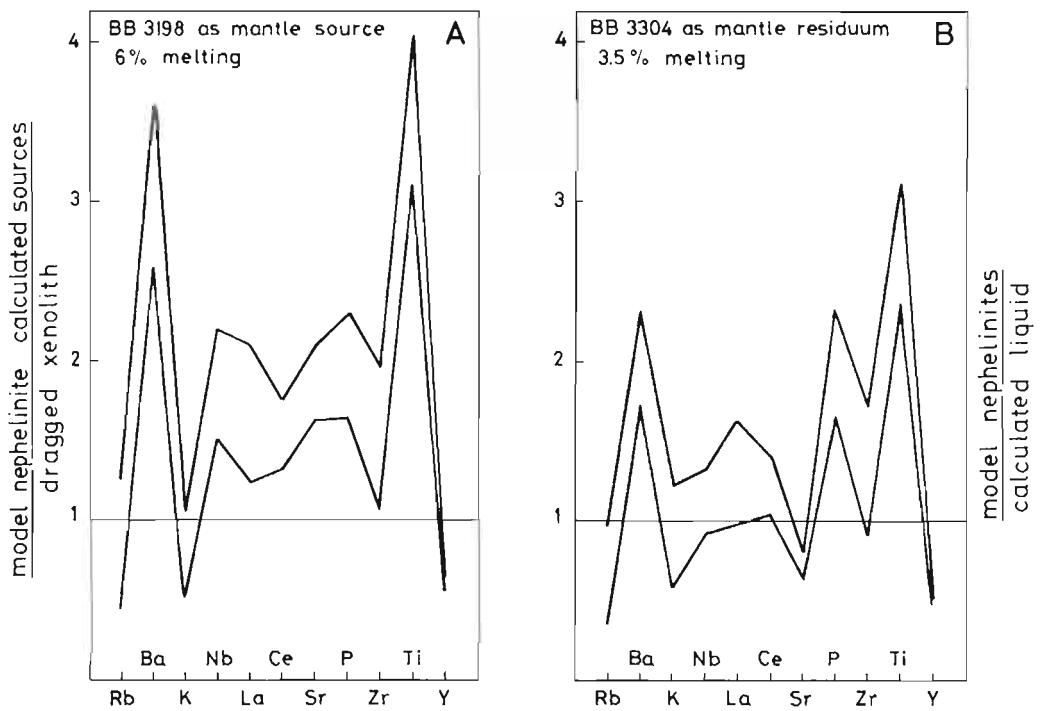

Fig. 8. A : spidergrams of calculated mantle source compositions relative to theoretical nephelinites ("model nephelinites" 13 to 16, Table 8) normalized to the composition of BB3198 mantle lherzolite (Table 5) assumed here as mantle source. B : spidergrams of theoretical nephelinites normalized to calculated liquid, assuming 3.5 % melting and the BB3304 harzburgite (Table 5) as residuum.

xenoliths. On the contrary, garnet-peridotite sources are preferred, because these types of source allow a simpler explanation for the strong and variable fractionation between LREE and HREE (variable amounts of garnet in the residua). Note that garnet-peridotite sources also require important enrichments in incompatible elements relative to a primordial mantle.

Incompatible element enrichment may be broadly associated with metasomatic processes involving fluids and/or small volume melts (*e.g.* Menzies *et al.*, 1987 ; Erlank *et al.*, 1987). Whatever the origin of these fluids, there is in agreement that the source was probably in the deeper parts of the lithosphere or upper asthenosphere, and that such fluids likely derived from volatile-rich alkaline melts.

Assuming an average heat flow value of 58 mW/m^2 for the Paranà Basin (Hamza, 1982) in Eocene times, and a peridotite solidus with $CO_2/(CO_2 + H_2)$ of 0.8 (Wyllie, 1987), volatile-rich fluids could be related to partially melted diapirs generated mainly at depths less than 200 km. Thus, a wide zone of mantle metasomatism may extend between the lower part of the lithosphere up to the solidus ledge (Wyllie, 1987). The existence of primary carbonates of mantle origin in the Asunción nephelinites suggests a CO_2-bearing peridotite source with some H_2O component. The small enrichment in Zr relative to Nb in the mantle source could be due to Zr-Nb decoupling occurring at a particular $CO_2/(CO_2 + H_2O)$ ratio (Watson, 1979 ; Haggerty *et al.*, 1986). Different H_2O-CO_2 proportions at different depths might explain the compositional differences among the Asunción nephelinites.

The "metasomatic" event(s) might be linked to the thermal anomaly responsible for the generation of the Paranà Basin flood tholeiites (*ca.* 140-120 Ma). It is interesting to note that the metasomatic processes responsible for the formation of the South African phlogopite-K richterite peridotites occurred 90-150 Ma ago, after the peak of basaltic flood volcanism in the Karoo province at *ca.* 190 Ma (Waters & Erlank, 1988).

R_0-$^{143}Nd/^{144}Nd$ variations (*cf.* Fig. 6) show that the flood basalts of the Paranà Basin (Cordani *et al.*, 1988 ; Piccirillo *et al.*, 1989) are related to mantle sources isotopically distinct from those of the nephelinites and enclosed mantle xenoliths.

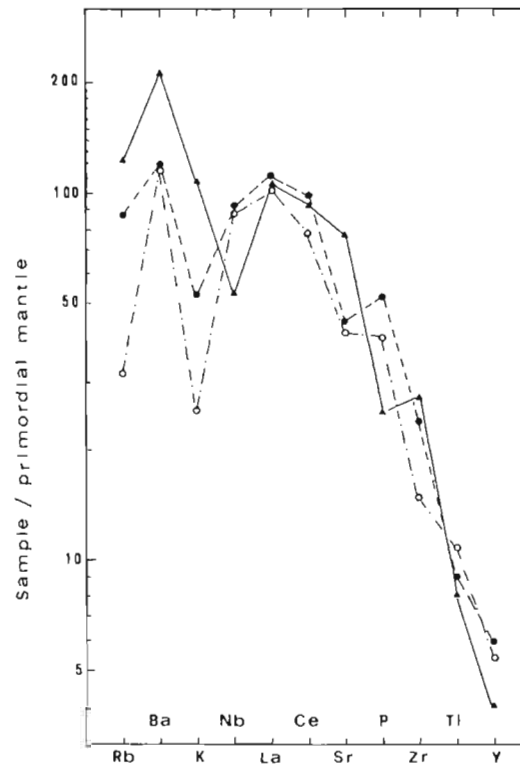

Fig. 9. Spidergrams of Asunción nephelinites (solid and open circles : Nemby and Cerro Patiño, respectively) and Mesozoic alkaline rocks (triangles : tephryte dykes of Sapucai area : De Min, unpublished data), normalized to primordial mantle (values from Nelson *et al.*, 1986, *i.e.* ppm : Rb = 0.69, Ba = 6.81, K = 240, Nb = 0.75, La = 0.71, Ce = 1.85, Sr = 23.7, P = 92, Nd = 1.37, Zr = 11.1, Ti = 1300, Y = 4.69).

We emphasize that the Sr isotope ratios of the Asunción nephelinites (R_0 = 0.7036 – 0.7039) are distinctly lower than those of the lower Cretaceous alkaline magmatism of Central-Eastern Paraguay (Sapucai-Ybituruzú area : 0.7073 ± 0.0003, age = 128 ± 8 Ma ; Bitschene, 1987), and even those of the adjoining Paranà flood basalts to the East (Ybyturuzú-Ciudad de Leste area : R_0 = 0.7059 ± 0.0002, age = 132 ± 12 Ma ; Bitschene, 1987 ; Piccirillo *et al.*, 1988). This indicates that the Tertiary alkaline magmatism of Paraguay originated from a more depleted mantle source, distinct from sources feeding the Cretaceous magmatism. Such mantle source differences might be responsible for the existence of a pro-

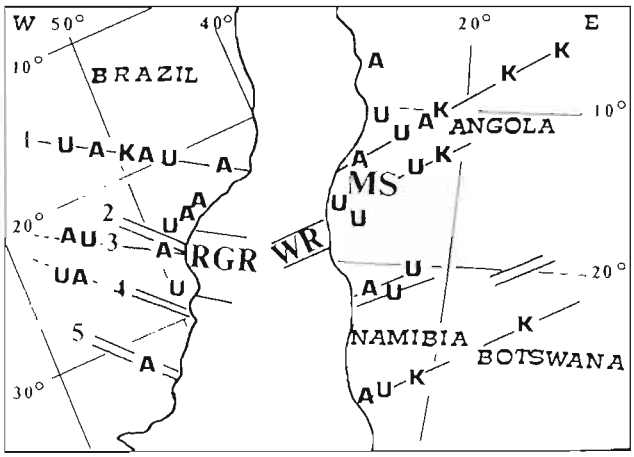

Fig. 10. Cretaceous Gondwanaland showing the opening of the South Atlantic Ocean and main lineaments across Africa and Brazil (1 : Araguaia-Paranaiba-Cabo Frio ; 2 : Ponta Grossa Arch ; 3 : Rio Piquiri ; 4 : Torres Syncline ; 5 : Rio Grande Arch). The major occurrences of alkaline complexes are shown (A, alkaline ; U, ultra-alkaline ; K, Kimberlite). RGR : Rio Grande Rise ; WR : Walvis Ridge ; MS : Mossamedes Swell. Modified after Le Bas (1987). Source data : Smith & Briden, 1977 ; Sadowski, 1987 ; Piccirillo *et al.*, 1989 ; Gomes *et al.*, 1990.

nounced negative Nb anomaly in the Cretaceous alkaline magmatism but not in the investigated Tertiary nephelinites (Fig. 9).

If reference is made to the distribution of alkaline and ultra-alkaline Mesozoic and Tertiary magmatism in SE-Brazil as well as in the Angola-Namibia counterpart (Fig. 10), we note that both show NW-SE and NE-SW trends, respectively. Notably, the alkaline magmatism trends transversally to the general N-S trend of the mid-ocean ridge, and does not follow the main structural grain of the crystalline basement. This indicates -as suggested by Sadowski (1987)- that the distribution of such Mesozoic-Tertiary alkaline magmatism was tectonically constrained by stress regime variations related to the opening of the South Atlantic, rather than by ancient structural lineaments.

Acknowledgements : The authors greatly benefitted from the critical review and helpful suggestions of Dr. A. Cundari.

Thanks are due to the Brazilian Agencies CNPq, FAPESP and FINEP and to Italian agencies CNR and MPI (40 %) for financial support. The CNR is acknowledged for financing the installation and maintenance of the microprobe laboratory at Cagliari University. The authors are indebted to Prof. Garbarino for assistance in microprobe work.

References

Bellieni, G., Brotzu, P., Comin-Chiaramonti, P., Ernesto, M., Melfi, A.J., Pacca, I.G., Piccirillo, E.M. & Stolfa, D. (1983) . Petrological and Paleomagnetic data on the Plateau basalt to rhyolite sequences of the Southern Paranà Basin (Brazil). *An. Acad. brasil. Ciênc.*, **55**, 355-383.

Bellieni, G., Comin-Chiaramonti, P., Marques, L.S., Martinez, L.A., Melfi, A.J., Nardi, A.J.R., Piccirillo, E.M. & Stolfa, D. (1986) : Continental flood basalt from the central-western regions of the Paranà plateau (Paraguay and Argentina) : petrology and petrogenetic aspects. *N. JB. Miner. Abh.*, **154**, 111-139.

Bitschene, P.R. (1987) : Mesozoischer und Kanozoischer anorogener magmatismus in Ostparaguay : arbeiten zur geologie und petrologie zweier Alkaliprovinzen. Ph.D. Dissertation, Heidelberg University, Heidelberg, 317 p. (unpublished).

Boettcher, A.L., O'Neill, J.R., Windom, K.E., Stewart, D.C. & Wilshire, H.G. (1979) : Metasomatism in the upper mantle and the genesis of kimberlites and alkali basalts. *In* "The mantle sample ; inclusions in kimberlites and other volcanics", F.R. Boyd and H.O.A. Meyer, ed. Proceedings of the II Intern. Kimberlite Conf., *Amer. Geophys. Union*, **2**, 173-182.

Bristow, J.W. (1984) : Nephelinites of the Lebombo and South-East Zimbabwe. *Spec. Publ. geol. S. Afr.*, **13**, 87-104.

Chen, J.C. (1971) : Petrology and chemistry of garnet lherzolite nodules in kimberlite from South Africa. *Am. Mineral.*, **56**, 2098-2110.

Comin-Chiaramonti, P., Demarchi, G., Girardi, V.A.V., Princivalle, F. & Sinigoi, S. (1986) : Evidence of mantle metasomatism and heterogeneity from peridotite inclusions of northeastern Brazil and Paraguay. E.P.S.L., **77**, 203-217.

Comin-Chiaramonti, P., Gomes, C.B., Piccirillo, E.M., Bellieni, G., Castillo A.M.C., Demarchi, G., Gallo, P. & Velasquez, J.C. (1990) : Petrologia do maciço alcalino de Acahay, Paraguay Oriental. *Rev. Bras. de Geociências,* in press.

Cordani, U.G., Civetta, L., Mantovani, M.S.M., Petrini, R., Kawashita, K., Hawkesworth, Taylor, P., Longinelli, A., Cavazzini G. & Piccirillo, E.M. (1988) : Isotope geochemistry of flood volcanics from the Paranà Basin (Brazil). *In* "The Mesozoic flood volcanism from the Paranà bazin (Brazil) . petrogenetic and geophysical aspects", E.M. Piccirillo and A. J. Melfi, ed. IAG-Usp, Sâo Paulo, Brazil, 157-178.

Dautria, J.M., Liotard, J.M., Cabanes, N., Girod M. & Briqueu, L. (1987) . Amphibole-rich xenoliths and host alkali basalts : petrogenetic constraints and implications on the recent evolution of the upper mantle beneath Ahaggar (Central Sahara, Southern Algeria). *Contrib. Mineral. Petrol.*, **95**, 133-144.

Degraff, J.M., Franco, R. & Orué, D. (1981) : Interpretación geofisica y geologica del valle de Ypacaray (Paraguay) y su formación. *Ass. Geol. Argent.*, **36**, 240-256.

De La Roche, H., Leterrier, P., Grandclaude, P. & Marchal, M. (1980) . A classification of volcanic and plutonic rocks using R1-R2 diagram and major-element analyses. Its relationships with current nomenclature. *Chemical Geol.*, **29**, 183-210.

Demarchi, G., Comin-Chiaramonti, P., De Vito, P., Sinigoi, S. & Castillo, C.A.M. (1988) : Lherzolite-dunite xenoliths from Eastern Paraguay . petrological constraints to mantle metasomatism. *In* "The Mesozoic flood volcanism from the Paranà basin (Brazil) : petrogenetic and geophysical aspects", E.M. Piccirillo and A.J. Melfi, ed. IAG-USP, Sâo Paulo, Brazil, 207-227.

Eby, N.G. & Mariano A.N. (1986) : Geology and geochronology of carbonatites peripheral to the Paranà basin, Brazil-Paraguay. *Carbonatite Symp.*, Ottawa, 13 p.

Eggler, D.H. (1978) : The effect of CO_2 upon partial melting of peridotite in the system Na_2O-CaO-Al_2O_3-MgO-SiO_2-CO_2 to 35 kb, with an analysis of melting in a peridotite-H_2O-CO_2 system. *Amer. Jour. Sci.*, **278**, 305-343.

Erlank, A.J., Waters, F.G., Hawkesworth, C.J., Haggerty, S.E., Allsopp, H.L., Rickard, R.S. & Menzies, M.A. (1987) : Evidence for mantle metasomatism in peridotite nodules from the Kimberley pipes, South Africa. *In* "Mantle Metasomatism", M.A. Menzies and C.J. Hawkesworth, ed. London Academic Press, 221-309.

Ewart, A. & Hawkesworth, C.J. (1987) : The Pleistocene-recent Tonga-Kermadec arc lavas : interpretation of new isotopic and Rare Earth data in terms of a depleted mantle source model. *J. Petrol.*, **28**, 495-530.

Faure, G. (1986) : Principles of Isotope Geology. IInd ed., Wiley & Sons, Inc., New York, 589 p.

Fodor, R.V., Mukasa, S.B., Gomes, C.B. & Cordani, U.G. (1989) : Ti-rich Eocene basaltic rocks, Abrolhos Platform, offshore Brazil, 18°S : Petrology with respect to South Atlantic magmatism. *J. Petrol.*, **30**, 763-786.

Frey, F.A. & Prinz, M. (1978) : Ultramafic inclusions from San Carlos, Arizona : petrological and geochemical data bearing on their petrogenesis. *E.P.S.L.*, **38**, 129-176.

Frey, F.A., Green, D.H. & Roy, S.D. (1978) : Integrated models of basalt petrogenesis : a study of quartz tholeiites to olivin melilites from South Eastern Australia utilizing geochemical and experimental petrological data. *J. Petrol.*, **19**, 463-513.

Gerlach, D.C., Stormer, J.C.Jr. & Mueller, P.A. (1987) . Isotopic geochemistry of Fernando de Noronha. *E.P.S.L.*, **85**, 129-144.

Gomes, C.B., Ruberti, E. & Morbidelli, L. (1990) : Carbonatite complexes from Brazil : a review. *J. South Am. Earth. Sci.*, **3**, 51-63.

Haggerty, S.E., Erlank A.J. & Grey, I.E. (1986) : Metasomatic mineral titanate complexing in the upper mantle. *Nature* **319**, 761-763.

Hamza, V.M. (1982) : Thermal structure of South American continental lithosphere during Archean and Proterozoic. *Rev. Bras. Geociènc.*, **12**, 149-159.

Hanson, G.N. (1977) : Geochemical evolution of the suboceanic mantle. *J. geol. Soc. London,* **134,** 235-253.

Harris, P.G., Reay, A. & White, I.G., (1967) : Chemical composition of the upper mantle. *J. Geophys. Res.*, **72**, 6359-6369.

Irving, A.J. (1978) : A review of experimental studies of crystal/liquid trace element partitioning. *Geochim. Cosmochim. Acta,* **42**, 743-770.

Le Bas, M.J. (1987) : Ultra-alkaline magmatism with or without rifting. *Tectonophysics,* **143**, 75-84.

— (1989) : Nephelinitic and basanitic rocks. *J. Petrol.*, **30**, 1299-1312.

Livieres, R.A. & Quade, H. (1987) : Distribución regionál y asentamiento tectonico de los complejos alcalinos del Paraguay. *Zbl. Geol. Paloont.*, **Teil I, H7/8**, 791-805.

Maaløe, S. & Prinzlau, I. (1979) : Natural partial melting of spinel lherzolite. *J. Petrol.*, **20**, 727-741.

Macgregor, I.D. (1977) Mafic and ultramafic xenoliths from the Kao Kimberlite pipe. *In* "Proc.

Second Int. Kimberlite Conf.", F.R. Boyd and H.O.A. Menzies, ed. 2, 156-172.

Menzies, M.A. & Murthy, V.R. (1980) : Mantle metasomatism as a precursor of the genesis of alkaline magmas. Isotopic evidence. *Am. Jour. Sci.*, **280A**, Jackson Volume, 622-638.

Menzies, M, Rogers, N.W., Tindle, A. & Hawkesworth, C.J. (1987) : Metasomatic and enrichment processes in lithospheric peridotites, an effect of asthenosphere-lithosphere interaction. *In* "Mantle Metasomatism", M.A Menzies and C.J. Hawkesworth, ed. London Academic Press, 313-359.

Mercier, J.C. (1980) : Single-pyroxene thermobarometry. *Tectonophysics*, **16**, 1-37.

Mercier, J.C. & Nicolas A. (1975) : Textures and fabrics of upper-mantle peridotites as illustrated by xenoliths from basalts. *J. Petrol.*, **16**, 454-487.

Nelson, D.R., McCulloch, M.T., Sun S-S. (1986) The origin of ultrapotassic rocks as inferred from Sr, Nd and P isotopes. *Geochim. Cosmochim. Acta*, **50**, 207-217.

Ottonello, G, Ernst, W.G., Joron, J.L. (1984) : Rare Earth and 3-d transition element geochemistry of peridotitic rocks : I) peridotite from Western Alps. *J. Petrol.*, **25**, 243-372.

Pearce, J.A. & Norry, M.J. (1979) : Petrogenetic implications of Ti, Zr, Y and Nb variations. *Contrib. Mineral. Petrol.*, **69**, 33-47.

Piccirillo, E.M., Civetta, L., Petrini R., Longinelli, A., Bellieni, G, Comin-Chiaramonti, P., Marques, L.S. & Melfi, A.J. (1989) : Regional variations within the Paranà continental flood basalt sequences as evidence for different mantle regions and variable crustal contamination. *Chemical. Geol.*, **75**, 103-122

Piccirillo E.M., Comin-Chiaramonti, P., Bellieni, G., Civetta, L., Marques, L.S., Melfi, A.J., Petrini, R., Raposo M.B. & Stolfa, D. (1988) : Petrogenetic aspects of continental flood basalt-rhyolite suites from the Paranà Basin (Brazil). *In* "The Mesozoic flood volcanism of the Paranà Basin : petrogenetic and geophysical aspects", E.M. Piccirillo and A.J. Melfi, ed. IAG-Usp, Sâo Paulo, Brazil, 179-205.

Pineau, F. & Mathez, E.A. (1990) : Carbon isotopes in xenoliths from the Hualalai Volcano, Hawaii, and the generation of isotopic variability. *Geochim. Cosmochim. Acta*, **54**, 217-227

Prinzhofer, A. & Allègre, C.J. (1985) . Residual peridotites and the mechanism of partial melting. *E.P.S.L.*, **74**, 251-256.

Roden, F.M. (1987) Rb/Sr and Sm/Nd ratios of metasomatic mantle ; implications for the role of metasomatized mantle in the petrogenesis of Na_2O-rich alkaline basalts. *In* "Mantle metasomatism and alkaline magmatism", E.M. Morris and J.D. Pasteris, ed., *Soc. Geol. Amer. Sp. p.*, **215**, 127-138.

Roden, M.H., Hart, S.R., Frey, F.A. & Melson, W.G. (1984) : Sr, Nd and Pb isotopic and REE geochemistry of St. Paul's Rocks : the metamorphic and metasomatic development of alkali basalt mantle source. *Contrib. Mineral. Petrol.*, **85**, 376-390.

Sadowski, G.R. (1987) : A possible relation between pulses of platform activation and plate kinematics. *Tectonophysics*, **143**, 43-58.

Smith, A.G. & Briden, J.C. (1977) · Mesozoic and Cenozoic paleocontinental Maps. Cambridge Univ. Press, 63 p.

Spera, F.J. (1984) : Carbon dioxide in petrogenesis III : role of volatiles in the ascent of alkaline magmas with special reference to xenolith-bearing mafic lavas. *Contrib. Mineral. Petrol.*, **88**, 217-232.

Villemant, B., Jaffrezic, H., Joron, J.L. & Treuil, M. (1981) : Distribution coefficients of major and trace elements : fractional crystallization in the alkali-basalt series of Chaîne du Puys (Massif Central, France). *Geochim. Cosmochim. Acta*, **45**, 1997-2016.

Waters, F.G. & Erlank, A.J. (1988) : Assessment of the vertical extent and distribution of mantle metasomatism below Kimberley, South Africa. *J. Petrol.*, Special Lithosphere Issue, p. 185-204.

Watson E.B. (1979) : Zircon saturation in felsic liquid : experimental result and applications to trace element geochemistry. *Contrib. Mineral. Petrol.*, **70**, 407-419.

Wilkinson, J.F.G. & Le Maître R.W. (1987) : Upper mantle amphiboles and micas and TiO_2, K_2O and P_2O_5 abundances and 100 Mg/(Mg + Fe^{2+}) ratios of common basalts and andesites · implications for modal mantle compositions. *J. Petrol.*, **28**, 37-73.

Wilshire, H.G. & Shervais, J.W. (1975) · Al-augite and Cr-diopside utramafic xenoliths in basaltic rocks from the Western United States. *Phys. Chem. Earth*, **9**, 257-272.

Wyllie, P.J. (1987) : Volcanic rocks : boundaries from experimental petrology. *Fortschr. Mineral.*, **65**, 249-284.

Zindler, A., Hart, S.R., Frey, F.A. & Jacobsen, S.P (1979) : Nd and Sr isotope ratios and REE abundances in Reykjanes Peninsula basalts : Evidence for mantle heterogeneity beneath Iceland. *E.P.S.L.*, **45**, 249.262.

Received 7 June 1990
Accepted 11 January 1991